Study on the Applicability of ESA Global Landcover in Wind Power Engineering

Jing Zhang[1,] *, Peirong Hu[1]

[1] Beijing RETEC New Energy Technology Co., Ltd., Beijing 100079,

zhangjing@bjretec.com, hupeirong@rkkj1.wecom.work

ABSTRACT:

Surface roughness is used as input data in the wind resource assessment process, which has a direct impact on the simulation of wind farm flow fields and the calculation of power generation. The ESA Global Landcover10m ground coverage dataset WorldCover 10m (2020) was introduced in the wind resource assessment process of three typical complex terrain projects in this paper, and the results were tested, yielding a high accuracy. The projects are located in the Northwest, Northeast, and Central China regions, and each project's met mast perform cross-forecasting in pairs. The wind flow field simulation results validate the key indicators such as wind speed, wind direction, wind frequency, and correlation, and then validate the power generation results. The final annual power generation calculation results are within 5% of the mean.

Keywords:

WorldCover, Roughness length, Landcover, Wind Resources

1 INTRODUCTION

Wind power is growing in popularity as people become more concerned about environmental protection and green energy. Last year, the global onshore wind market added 68.8 GW, with China accounting for 52%. China's commitment to expanding the role of renewables in its energy mix, with the goal of renewable energy contributing more than 80% of total new electricity consumption by the end of the 14th Five-Year Plan (2021-2025)[1].

The assessment of wind resources in China has gradually become more refined. A more accurate and reliable assessment of wind resources will aid in the development of wind resources, saving money and increasing output. As a result, it is extremely important and necessary to improve the accuracy and reliability of resource evaluation. Engineers must use cutting-edge technology and resources to create high-resolution, high-precision wind resource maps in wind farms in order to build wind power projects.

At the moment, the most commonly used ground cover products in wind resource assessment are the National Aeronautics and Space Administration's (NASA) GeocoverLC 90m resolution data set (2009) [2], the European Space Agency's (ESA) Copernicus Global Land Service (CGLS) 100-meter land cover data set (2015-2019) [3], and the National Basic Geographic Information Center of China's Globeland 30[4]. The global land cover data with 10m resolution released by ESA in 2020 will be used in this paper to calculate the roughness length, which will be used to simulate the wind farm flow field. The projects in China's northeast, northwest, and central regions were chosen to simulate the flow field, and the results were tested. The research presented in this paper is expected to serve as a reference for wind resource assessment.

2 OVERVIEWS

2.1 GROUND COVERAGE DATA

The release of a global land cover (GLC) product with a resolution of 10m in 2020 in October, 2021 is the key achievement of the European Space Agency's WorldCover project. This product contains 11 land cover categories and has been independently verified based on Sentinel-1 and Sentinel-2 data, with an overall global accuracy of 74.4% and an overall accuracy of 80.5% in Asia. The accuracy of the categories of tree cover and snow, farmland, water body, and bare/sparse vegetation is higher, at more than 80%. The accuracy of grassland and architecture is moderate, whereas shrub, wetland, and moss/lichen accuracy are low. Bryophytes, lichens, and grasslands are overestimated, while trees are underestimated[5].

Esri's Landcover coverage, which is also based on Sentinel satellite data at 10m resolution, includes nine types, including water, grassland, ice, and snow, with an overall accuracy of 85%[6]. Despite the fact that LandCover appears to have higher overall accuracy, studies have shown that WorldCover has higher accuracy and LandCover accuracy is relatively lower at smaller cell resolution ($100m^2$)[7].

The National Basic Geographic Information Center of China's land cover data GlobeLand30 (2020) is widely used in the current wind resource assessment work. GlobeLand30 products cover an area of 80 °S-80 °N with a resolution of 30m. Ground cover is classified into ten types, including cultivated land, forest, water, and artificial cover. Among them, the minimum classification accuracy of six types, including cultivated land and forest, is controlled at or above 70%, while the lowest classification accuracy of four types, including water bodies and artificial cover, is controlled at or above 80%. In China, the precision of the data set is 80.4% [8][9].

2.2 DATA SELECTION

Project A is located in Northwest China in the N47E086 area, at an altitude of more than 500 meters and on relatively flat terrain. Gobi land dominates the west side of the project area, while vegetation and construction land dominate the east side. Two 100m met mast are part of the project. WorlaCover and GlobeLand30 data are more similar in general, with some differences in wetland and cultivated land. When compared to satellite maps, WorldCover clearly shows more ground details, while LandCover has a large difference with other data, and the information integrity of grassland and shrubs is relatively low (Figure 1).

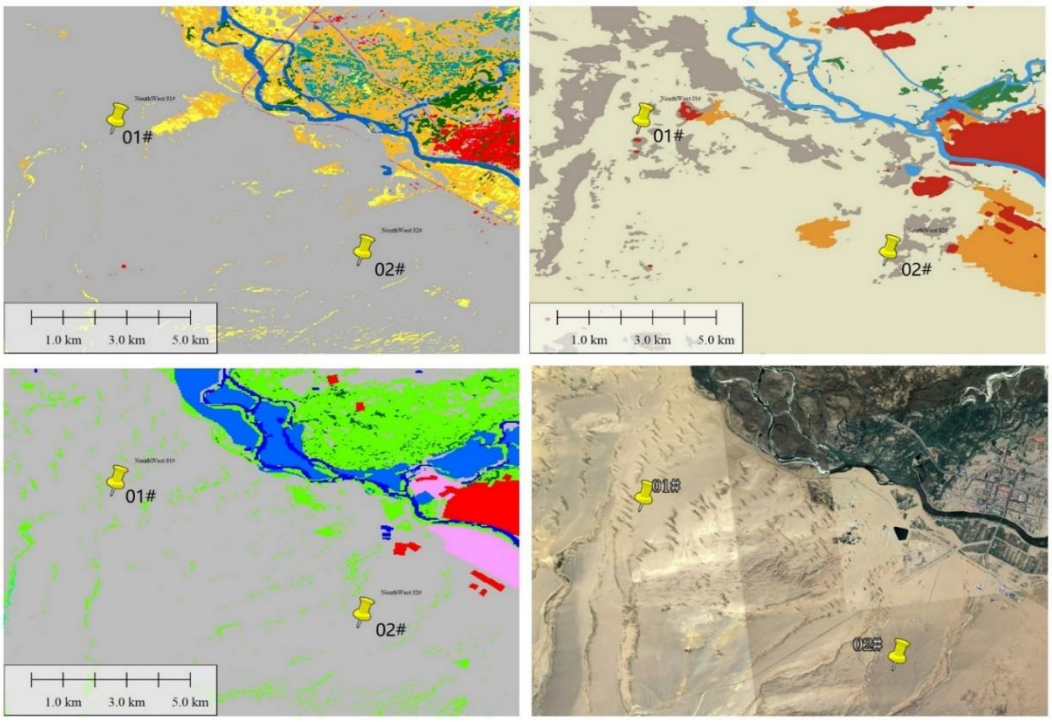

Figure 1 Comparative schematic diagram of ground coverage data of project A in Northwest China
The top left is WorldCover, the top right is LandCover, the bottom left is GlobeLand30, and the bottom right is Google Earth satellite map.

Project B is located in Central China in the N26E110 area, on the eastern edge of the Yunnan-Guizhou Plateau. It is characterized by hilly terrain and has an elevation of more than 1,000 meters. Two 100m met masts are available. Figure 2 also shows that the three land cover datasets have a high degree of approximation. When compared to the satellite map, it is clear that WorldCover reflects more ground details with high accuracy. LandCover depicts the majority of the land cover but is still lacking in more detailed information.

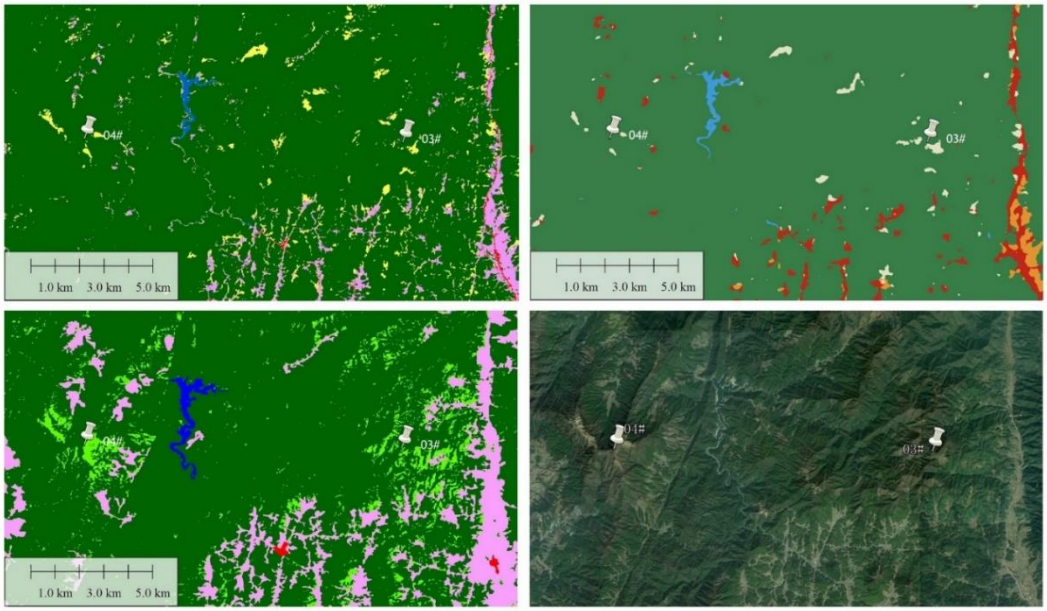

Figure 2 Comparative schematic diagram of ground coverage data of project B in Central China
The top left is WorldCover, the top right is LandCover, the bottom left is GlobeLand30, and the bottom right is Google Earth satellite map.

Project C in Northeast China is located at an altitude of 900-1000 meters in the N42E120 area. It is

situated on the border between the Greater Khingan Mountains and the Songnen Plain. It is a low-mountain setting. There are three 100-meter wind-measuring towers, with the 05# wind-measuring station at an altitude of 1137 meters. The 06# met mast is located at an altitude of 986m, while the 07# met mast is located at an altitude of 1119m. According to the comparison chart (Figure 3), WorldCover and GlobeLand30 are very similar. According to the data, the project site is mostly cultivated land and grassland, with some woodlands and buildings (villages). The farmland built in accordance with the mountain is clearly visible. The ridge's direction is consistent with the satellite map.

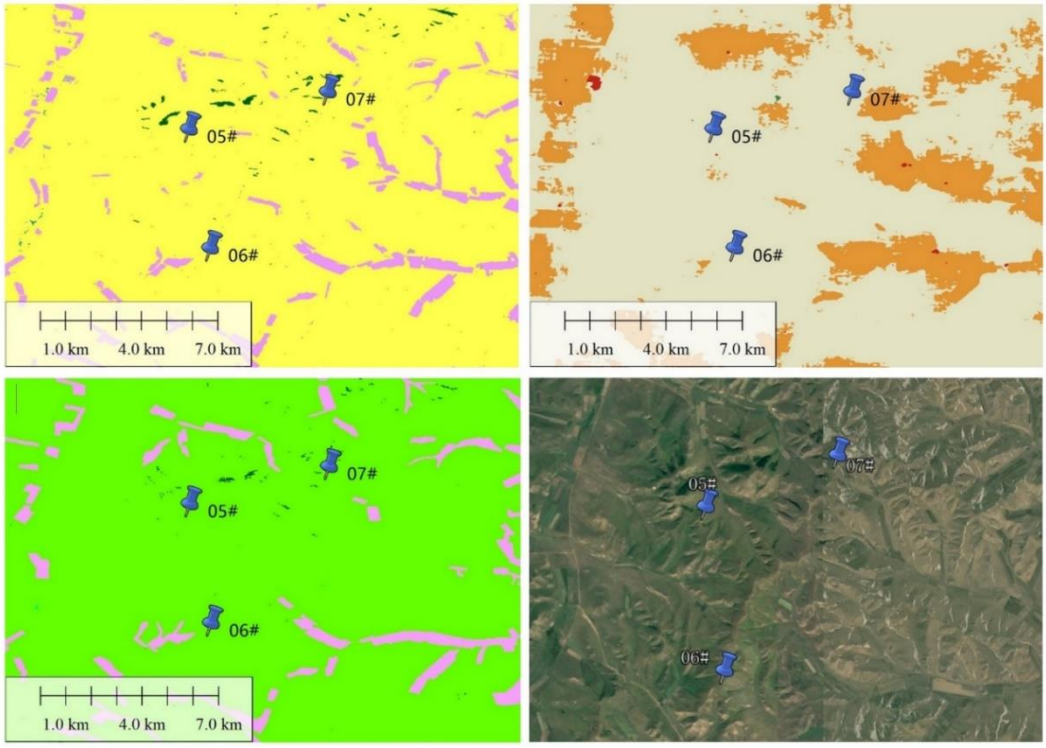

Figure 3 Comparative schematic diagram of ground coverage data of project C in Northeast China
The top left is WorldCover, the top right is LandCover, the bottom left is GlobeLand30, and the bottom right is Google Earth satellite map.

2.3 RESEARCH METHOD

2.3.1 Roughness length making

To use the ESA WorldCover ground cover data set in wind resource assessment, first establish the printing relationship between ground cover data and surface roughness. The mapping relationship between ground cover and roughness length was established using the European Wind Energy Atlas[10] and the new European Wind Energy Atlas[11], and the roughness length value was adjusted based on the actual local conditions.

Table 1 Roughness Length

Code	Land Use Land Cover Class	EWA Roughness Classification	EWA Roughness Length (m)	Modified Roughness Length (m), A	Modified Roughness Length (m), B	Modified Roughness Length (m), C
10	Tree cover	2.5	0.65	0.85	0.85	0.7
20	Shrubland	1.5	0.15	0.15	0.25	0.03
30	Grassland	1	0.03	0.1	0.01	0.03

40	Cropland	1	0.05	0.1	0.05	0.07
50	Built-up	3	1	0.5	0.55	0.15
60	Bare	1	0.01	0.05	0.01	0.03
70	Snow and ice	0	0.001	0.001	0.001	0.001
80	Water	0	0.0001	0.001	0.0001	0.001
90	Wetland	1	0.03	0.3	0.05	0.3
95	Mangroves	2	0.15	0.15	0.15	0.15
100	Moss and lichen	1	0.01	0.01	0.01	0.01

2.3.2 Software emulation

Because ground roughness affects wind flow field simulation and power generation calculation as input data, this paper will verify these two aspects.

In previous research, the mass conservation wind flow field model of Openwind software was validated, and the results showed that its error was comparable to, if not lower than, that of other similar software products[12]. In this paper, Openwind is still used to simulate the wind flow field.

Compare the wind speed and direction obtained from the simulation, and then use the power curve of the GW165-5.0MW wind turbine to calculate and compare power generation.

3 RESULT AND ANALYSIS

3.1 PROJECT ANALYSIS IN NORTHWEST CHINA

In the Northwest China project, 01# wind measurement data was used to extrapolate 02# data, and 02# data was used to extrapolate 01# data, and the two sets of Synthetic data obtained were compared and analyzed with the measured data. Table 1 displays the results. Analysis of correlations between fitted and measured data for each height layer, including two met masts. The data show that the Pearson correlation coefficient r between the fitted data and the measured data is between 0.875 and 0.933, indicating that the fitted data's fluctuation trend is essentially consistent with the fluctuation trend of the measured data, and the correlation is very good.

Table 2 also displays the calculated error results between the fitted and measured data. The average wind speed error between the fitted and measured data is found to be relatively low, with an average absolute value of 2.47%. Some are excessively large. The largest error is 6.63% and the wind speed difference is 0.521m/s between the fitting wind speed at the height of 80m of the 01#met mast and the measured wind speed.

At the same time, the F test was performed in pairs for the fitted data and the measured data, and when compared using the test method described in the previous section, it was discovered that the variance of the fitted data at 30m and 90m of the 02#met mast and the measured data showed significant differences, indicating that there is a large difference in the distribution of wind speed between the two sets of Synthetic data and the measured data. The F test of the 01#met mast Synthetic data and the measured data all show consistency of variance, and it can be assumed that the distribution of the 01#met mast Synthetic data in each wind speed segment is also similar to the measured data.

Table 2 Wind data simulation results for the Northwest Project

		10m	30m	50m	80m	90m	100m
01# is predicted by 02#	Predicted	5.814	6.822	7.406	7.341	8.014	8.39
	Actual	5.921	6.654	7.295	7.862	8.103	8.249
	Error (%)	-1.81%	2.52%	1.52%	-6.63%	-1.10%	1.71%
	r	0.912	0.875	0.909	0.936	0.902	0.933
	P-value	0.844	0.162	0.473	0.325	0.241	0.285
	Number	51746	52278	52263	52331	52352	52299
02# is predicted by 01#	Predicted	6.354	7.211	7.65	8.539	8.282	8.185
	Actual	6.518	7.466	7.828	8.363	8.299	8.509
	Error (%)	-2.51%	-3.42%	-2.27%	2.10%	-0.21%	-3.81%
	r	0.918	0.914	0.913	0.915	0.907	0.933
	P-value	0.949	0.037	0.225	0.672	0.018	0.282
	Number	52040	52225	52133	52286	52307	52344

According to the results analysis, the error decreases with increasing height near the surface (10m~30m), whereas at a higher height from the surface, the error fluctuates with increasing height (Figure 4), indicating that the error increases at first and then decreases with increasing height.

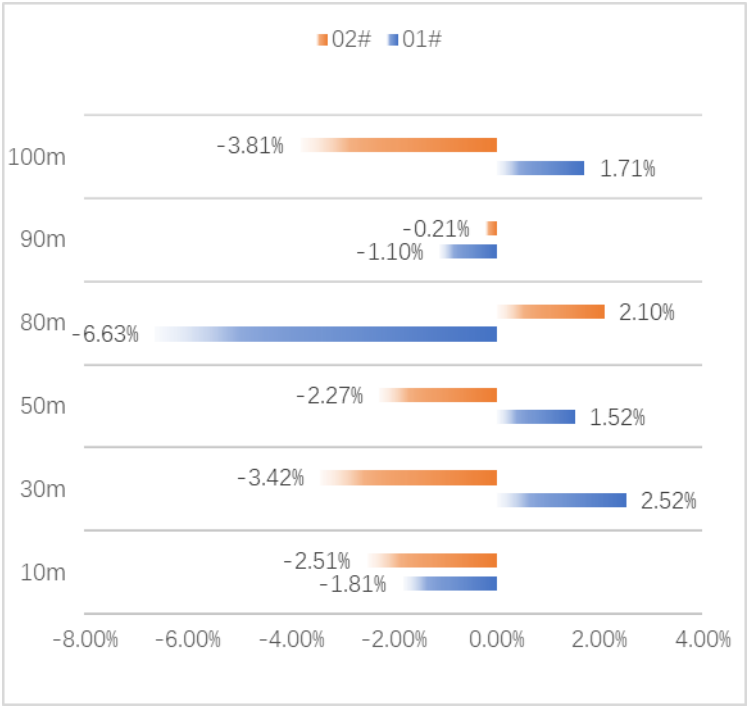

Figure 4 Northwest Project Error Statistics for Simulated Wind Speed Data

As shown in Figures 5, the 10m Synthetic data and measured data from the twomet masts are counted by sectors to form a wind direction rose diagram. The 01#met mast's main wind directions are ESE and SE, and the measured frequencies of the two main wind directions are 26.33% and 7.89%, respectively, for a total main wind direction frequency of 34.22%. The fitting frequency is 19.27% and 12.46%, respectively, for a total main wind direction frequency of 31.73%. The main wind directions of the 02#met mast are ESE and SE, and the measured frequencies are 17.65% and 19.97%. The fitting wind direction of 01#met mast

and 02#met mast 10m is in good agreement with the measured wind direction.

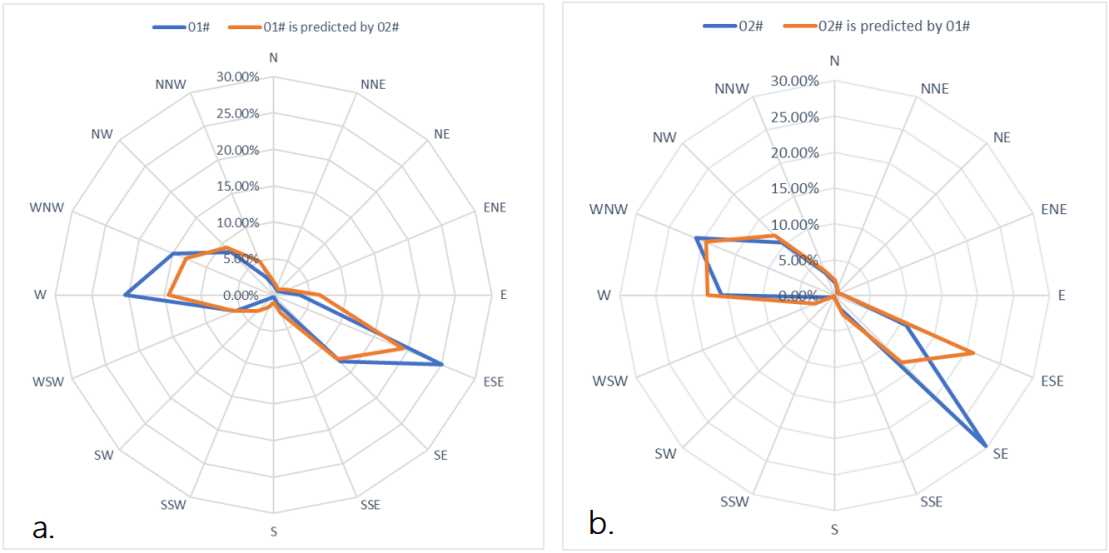

Figure 5 Met mast wind direction rose (5a. 01#, 5b. 02#)

Following that, we validate through power generation. Point 01# calculates the annual power generation of 23374MWh from the measured data and the annual power generation of 24443MWh from the Synthetic data, with a 4.6% deviation. Point 02# calculates the annual power generation of 24267MWh from the measured data and the annual power generation of 23912MWh from the Synthetic data, with a 1.5% deviation.

3.2 PROJECT ANALYSIS IN CENTRAL CHINA

The data from each layer of the Central China project's 03#met mast and the data from each layer of the 04#met mast are interpolated with the data from the same height layer to form the result table 3. The data show that the Pearson correlation system r value for the fitted data of the two met masts and the measured data are in the range of 0.616-0.817, indicating a strong correlation between the fitted data and the measured data. Except for Tower 3#'s 80m data correlation of 0.616, the data correlations of the other layers are all greater than 0.7, indicating a good correlation.

Table 3 Wind data simulation results for the Central Project

		10m	30m	50m	70m	80m
03# is predicted by 04#	Predicted	3.905	5.076	5.353	5.447	5.500
	Actual	3.801	5.149	5.486	5.673	5.730
	Error (%)	2.74%	-1.41%	-2.43%	-4.00%	-4.00%
	R	0.719	0.768	0.787	0.817	0.616
	P-value	0.935	0.394	0.079	0.183	0.002
	Number	50166	50185	50064	50035	50296
04# is predicted by 03#	Predicted	6.541	6.625	6.690	6.664	6.781
	Actual	6.893	7.021	7.120	7.167	6.406
	Error (%)	-5.11%	-5.63%	-6.04%	-7.02%	5.85%
	R	0.773	0.745	0.788	0.802	0.793
	P-value	0.005	0.092	0.327	0.627	0.005

Number	50069	50086	50064	49931	50263

According to Figure 6, the wind speed error between the Synthetic data of 03# and 04# met mast and the measured data is within 7.5%, with an average absolute value of 4.5%.

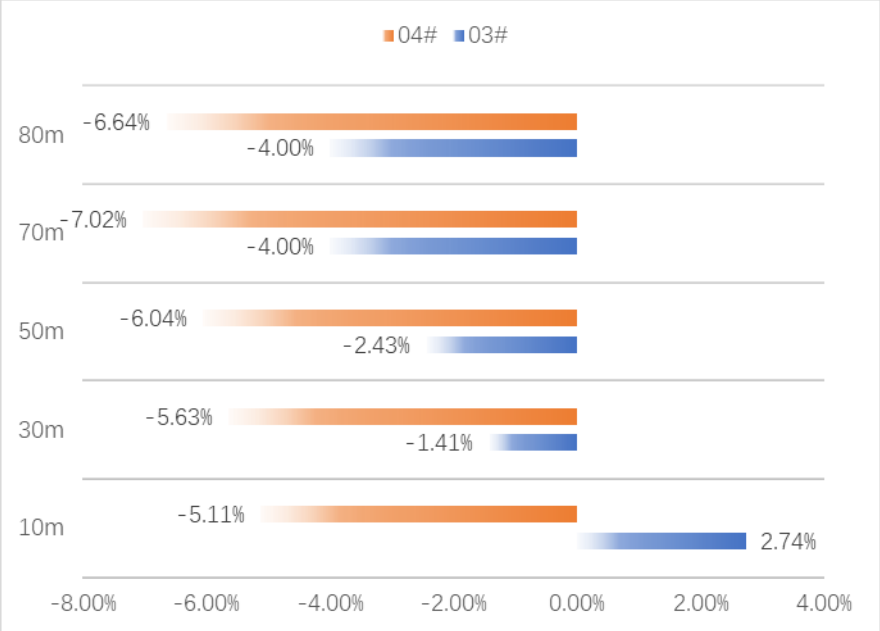

Figure 6 Central Project Error Statistics for Simulated Wind Speed Data

Table 3 and Figure 6 show that the 04# Synthetic data error is relatively higher, with an average absolute value of 6.1%. When the measured data of 03# is compared to the measured data of 04#, the correlation between the measured data of 03# met mast and the measured data of 04# met mast is 0.754, which is a good correlation. The average wind speed of each layer of the 03# met mast's measured data is low. When the 03#met mast data is used to extrapolate the 04#met mast data, the wind speed of each layer of the measured data of the 04#met mast is underestimated.

Figures 7 show rose diagrams of measured and fitted wind directions at 10m height of met mast03# and 04# in Central China. At 10m from the 03#met mast, the main wind directions are ENE, E, ESE, the measured frequencies are 11.72%, 19.43%, and 10.37%, and the total main wind direction frequencies are 41.53%; the fitting frequencies are 15.42%, 19.73%, and 7.61%, and the total main wind direction frequencies are 41.53%. The frequency of wind direction is 42.76%. The 10m main wind directions of the 04#met mast are S, SSW, and SW; the measured frequencies are 9.51%, 17.52%, and 10.73%, respectively, and the total main wind direction frequency is 37.76%; the fitting frequencies are 9.56%, 19.58%, and 9.06%, respectively, and the total main wind direction frequency is 37.76%. The percentage is 38.2%. This demonstrates that the fitted wind direction agrees well with the measured wind direction.

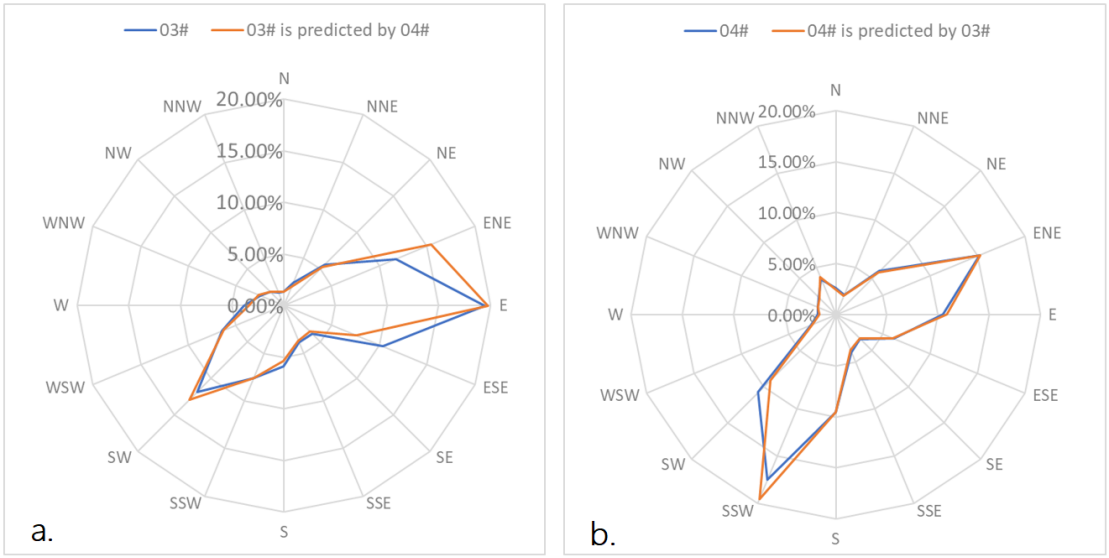

Figure 7 Met mast wind direction rose（7a. 03#, 7b. 04#）

The power generation results are validated after comparing and verifying wind data. Point 3# calculates the annual power generation of 12758MWh from the measured data and the annual power generation of 12258MWh from the Synthetic data, with a 3.9% deviation. The annual power generation calculated using the measured data at point 4# is 15412MWh, while the annual power generation calculated using the Synthetic data is 15303MWh, with a 0.7% deviation.

3.3 PROJECT ANALYSIS IN NORTHEAST CHINA

The project in Northeast China includes three wind-measuring towers that are cross-checked in pairs, and the results are presented in Tables 3, 4, and 5. The data error is controlled within 9%, the average absolute value of the error is 2.23%, and the deviation between the Synthetic data and the measured wind speed is small. The data's correlation system r value ranges from 0.798 to 0.901, indicating a strong correlation between the fitted and measured data. The F test was used on each set of data to determine whether or not the variance difference was significant.

Table 4 shows the cross-check results for the 05# and 06# met masts. Both the 05# Synthetic data extrapolated from the 06# wind measurement data and the 06# Synthetic data obtained from the 05# data extrapolation performed admirably in terms of wind speed error, correlation, and F test. It is worth noting that the Synthetic data of 06# obtained by extrapolating the measured data of 05# are generally, to varying degrees, underestimated. When combined with the TD results of terrain differences, it is possible to conclude that the terrain has a significant impact on this phenomenon. The altitude of the 05# met mast is 1137m, and the altitude of the 06# met mast is 986m, and the measured data shows that the wind speed of each altitude layer of the 06# met mast is greater than the wind speed of each test layer of the 05# met mast. The wind speed of the 06# met mast was underestimated due to the model's influence.

Table 4 Wind data simulation results for the Northeast Project (05#~06#)

		30m	70m	80m	90m	100m
05# is predicted by 06#	Predicted	7.008	7.503	7.628	7.804	7.906
	Actual	6.824	7.421	7.577	7.761	7.888
	Error	2.70%	1.10%	0.67%	0.54%	0.22%
	R	0.811	0.827	0.847	0.853	0.856
	P-value	0.685	0.623	0.889	0.673	0.508

	Number	51518	51483	51469	51480	51482
06# is predicted by 05#	Predicted	8.655	9.155	9.323	9.415	9.500
	Actual	9.134	9.515	9.468	9.567	9.614
	Error	-5.25%	-3.78%	-1.53%	-1.58%	-1.19%
	R	0.798	0.826	0.866	0.872	0.870
	P-value	0.491	0.836	0.693	0.742	0.578
	Number	51867	51458	51436	51459	51415

Table 5 displays the cross-check results of the 05# and 07# met masts. The Synthetic data from the two met masts correlated well with the actual measurements, and both passed the F test, indicating that there was no significant difference in variance. The Synthetic data from the 07# met mast extrapolated from the data from the 05# met mast has a maximum error of 8.65% with the measured data, and the wind speed difference is 0.884m/s. At each altitude, the fitted wind speed is understated to varying degrees.

Table 5 Wind data simulation results for the Northwest Project (05#~07#)

		30m	70m	80m	90m	100m
05# is predicted by 07#	Predicted	7.141	7.646	7.645	7.821	7.929
	Actual	6.824	7.421	7.577	7.761	7.888
	Error	4.64%	3.03%	0.89%	0.77%	0.52%
	R	0.806	0.825	0.838	0.846	0.853
	P-value	0.836	0.781	0.347	0.191	0.517
	Number	51962	51863	51839	51933	51870
07# is predicted by 05#	Predicted	9.338	9.380	9.997	10.069	10.119
	Actual	10.222	10.141	10.251	10.312	10.288
	Error	-8.65%	-7.51%	-2.48%	-2.36%	-1.64%
	R	0.820	0.839	0.856	0.861	0.848
	P-value	0.383	0.975	0.910	0.532	0.856
	Number	51867	51858	51859	51912	51855

Table 6 forms the cross-check results between 06# wind data and 07# wind data. he Synthetic data from the two met masts correlated well with the actual measurements, and both passed the F test, indicating that there was no significant difference in variance. The Synthetic data from the 07# met mast extrapolated from the data from the 06# met mast has a maximum error of 3.68% with the measured data, and the wind speed difference is 0.0.376m/s. At each altitude, the fitted wind speed is understated to varying degrees.

Table 6 Wind data simulation results for the Northwest Project (06#~07#)

		30m	70m	80m	90m	100m
06# is predicted by 07#	Predicted	9.435	9.829	9.490	9.587	9.642
	Actual	9.134	9.515	9.468	9.567	9.614

	Error	3.30%	3.30%	0.24%	0.21%	0.28%
	R	0.899	0.894	0.899	0.901	0.900
	P-value	0.895	0.845	0.776	0.989	0.663
	Number	51594	51501	51442	51529	51473
07# is predicted by 06#	Predicted	9.846	9.771	10.208	10.271	10.242
	Actual	10.222	10.141	10.251	10.312	10.288
	Error	-3.68%	-3.65%	-0.42%	-0.40%	-0.44%
	R	0.895	0.889	0.896	0.895	0.895
	P-value	0.429	0.256	0.388	0.680	0.237
	Number	51583	51545	51503	51516	51515

The cross-validation results of Project C in Northeast China show that the overall error is kept within a small range, and the error decreases with increasing height, whereas the error obtained by near-surface cross-validation is larger and more affected by surface coverage.

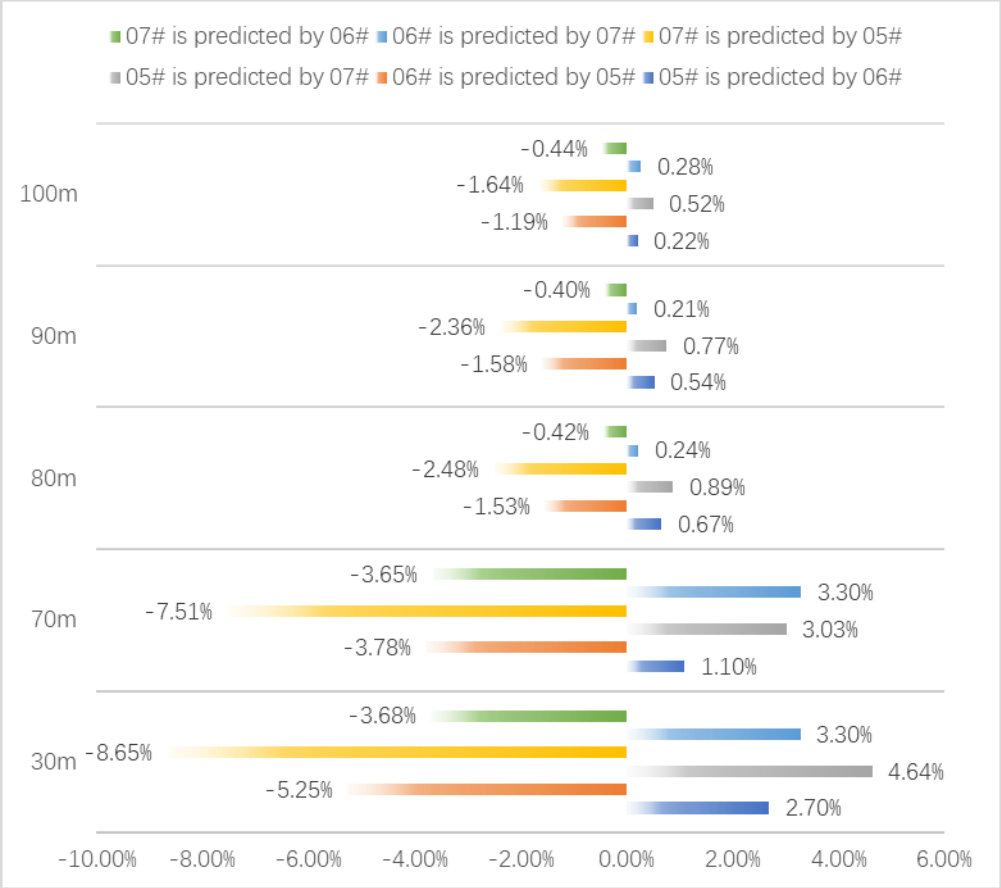

Figure 8 Northeast Project Error Statistics for Simulated Wind Speed Data

The measured frequency of the main wind direction WNW of the 05# wind data is 16.56%, and the measured frequency of the NW is 17.7%, for a total of 34.26%. The WNW frequency of 05# Synthetic data predicted by 06# wind measurement data is 17.97%, the NW frequency is 15.81%, and the total is 33.78%. According to the 07# wind measurement data, the 05# Synthetic data WNW frequency is predicted to be 17.19%, the NW frequency is 16.18%, and the total is 33.37%. The measured frequency of the main wind direction WNW is 19.62%, and the measured frequency of the NW is 17.06%, for a total of 36.68%. The WNW and NW frequencies of the 06# Synthetic data predicted by the 05# wind measurement data are

18.08% and 19.10%, respectively, for a total of 37.18%. The WNW frequency of 06# Synthetic data is predicted to be 19.45%, and the NW frequency is 17.51%, for a total of 36.96% based on the wind measurement data of 07#. The measured frequency of the main wind direction WNW is 19.69%, and the measured frequency of the NW is 17.4%, for a total of 37.09%. The measured frequency of the main wind direction WNW of 07# wind measurement data is 19.69%, and the measured frequency of the NW is 17.4%, for a total of 37.09%. The WNW frequency of 07# Synthetic data predicted by 05# wind measurement data is 18.15%, the NW frequency is 18.48%, and the total is 37.62%. According to the 06# wind measurement data, the 07# Synthetic data WNW frequency is predicted to be 19.68%, the NW frequency is 17.18%, and the total is 36.86%.

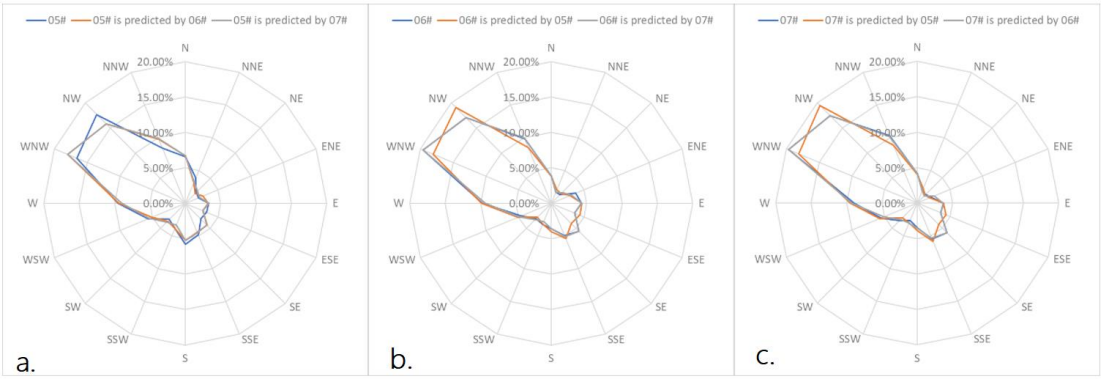

Figure 9 Met mast wind direction rose (9a.05#, 9b.06# and 9c.07#)

Finally, the results of the power generation are verified. The 5# point uses the measured data to calculate the annual power generation of 22802MWh; the annual power generation calculated by using the 6# data to fit the 5# data is 22907MWh, with a deviation of 0.46%; and the annual power generation calculated by using the 7# data to fit the 5# data is 22907MWh, with a deviation of 0.46%. The value is 23286MWh, and the standard deviation is 2.1%. The annual power generation calculated using the measured data at the 6# point is 27365MWh, and the annual power generation calculated using the 5# data to fit the 6# data is 27247MWh, with a deviation of 0.43%; the annual power generation calculated using the 7# data to fit the 6# data is 27247MWh, with a deviation of 0.43%; and the annual power generation calculated using the 8# data to fit the 6# data is 27365MWh. The value is 27949MWh, and the standard deviation is 2.1%. The 7# point uses measured data to calculate annual power generation of 29808MWh; the annual power generation calculated by fitting the 5# data to the 7# data is 29036MWh, with a deviation of 2.6%; and the annual power generation calculated by fitting the 6# data to the 7# data is 29036MWh, with a deviation of 2.6%. The amount is 29172MWh, and the standard deviation is 2.1%.

4 CONCLUSION

In this paper, the ESAGlobalLandcover10m ground cover data set WorldCover10m (2020) is introduced in the process of wind resource evaluation of three typical complex terrain projects, and the results are tested and high accuracy is obtained.

Correlation r validates the fitted data's consistency with the fluctuation trend of the original data.

The deviation of the average wind speed decreases with altitude, and the deviation of the Northeast Project occurs at a height of 10m, which is consistent with the fact that the wind is more affected by surface cover closer to the ground.

The 04# wind measurement data from Central China has negative shear at the upper level, and the simulated data failed to reveal the flaws, which is a limitation of the existing model. The negative shear may be caused by the low-level jet stream when combined with the site topography and climate conditions.

The deviation of power generation results is less than 5%, which has a good guiding effect on engineering construction.

Based on the above test results, WorleCover has a high potential for use in wind power projects.

REFERENCE

[1]. Council, G. W. E. (2023). GWEC Global Wind Report 2023. Global Wind Energy Council: Brussels, Belgium.

[2]. Cunningham, D., Melican, J. E., Wemmelmann, E., & Jones, T. B. (2002, July). GeoCover LC‐A moderate resolution global land cover database. In ESRI International User Conference.

[3]. Buchhorn, M., Lesiv, M., Tsendbazar, N. E., Herold, M., Bertels, L., & Smets, B. (2020). Copernicus global land cover layers—collection 2. Remote Sensing, 12(6), 1044.

[4]. National Geomatics Center of China. (2014). 30-meter Global Land Cover Dataset（GlobeLand30）Product Description. Beijing：National Geomatics Center of China

[5]. ESA 2021 WorldCover Product Validation Report v1.0 Chapter 3.1 Statistical Accuracy Assessment

[6]. Karra, K., Kontgis, C., Statman-Weil, Z., Mazzariello, J. C., Mathis, M., & Brumby, S. P. (2021, July). Global land use/land cover with Sentinel 2 and deep learning. In 2021 IEEE international geoscience and remote sensing symposium IGARSS (pp. 4704-4707). IEEE.

[7]. Venter, Z. S., Barton, D. N., Chakraborty, T., Simensen, T., & Singh, G. (2022). Global 10 m Land Use Land Cover Datasets: A Comparison of Dynamic World, World Cover and Esri Land Cover. Remote Sensing, 14(16), 4101.

[8]. Chen, J., Chen, J., Liao, A., Cao, X., Chen, L., Chen, X., ... & Mills, J. (2015). Global land cover mapping at 30 m resolution: A POK-based operational approach. ISPRS Journal of Photogrammetry and Remote Sensing, 103, 7-27.

[9]. Xie, H., Wang, F., Gong, Y., Tong, X., Jin, Y., Zhao, A., ... & Liao, S. (2022). Spatially Balanced Sampling for Validation of GlobeLand30 Using Landscape Pattern-Based Inclusion Probability. Sustainability, 14(5), 2479.

[10]. Troen, I. E. L. P., & Lundtang Petersen, E. (1989). European wind atlas.

[11]. Dörenkämper, M., Olsen, B. T., Witha, B., Hahmann, A. N., Davis, N. N., Barcons, J., ... & Mann, J. (2020). The making of the new european wind atlas–part 2: Production and evaluation. Geoscientific model development, 13(10), 5079-5102.

[12]. Jing Zhang, Jingwen Yang, Xianyang Wang (2021). Research into the Use of Wind Flow Models in Various Topographies. Hydropower and new energy, 35(9), 22-25. (In Chinses)